Revista de Metalurgia
January-March 2020, 56 (1), e159
ISSN-L: 0034-8570
https://doi.org/10.3989/revmetalm.159

# Quasi-static and dynamic analysis of single-layer sandwich structures of APM foam spheroid elements in-situ foamed with marble

José M. Ruiz-Román[a], Alejandro Sánchez de la Muela[a], Luis E. G.Cambronero[a], Íñigo Ruiz-Bustinza[a,✉]

[a]Department of Geological and Mining Engineering, School of Mining and Energy Engineering, Universidad Politécnica de Madrid, C/ de Ríos Rosas, 21, 28003 Madrid 28003, Spain

(✉ Corresponding author: inigo.rbustinza@upm.es)

Submitted: 25 June 2019; Accepted: 22 January 2020; Available On-line: 15 June 2020

**ABSTRACT:** In the present investigation, an experimental design of hybrid structures based on advanced pore morphology (APM) Al foam spheroid elements is studied. The energy absorption capacities of three configurations is assessed for both quasi-static and dynamic compressive loads. To this end experimental tests were performed by means of a universal testing machine using a 100 kN load cell (accuracy of 0.1%) and a drop weigh tower in a range of impactor masses varying from 2.2 to 23.12 Kg. The three types of samples explored are the following: foam spheroid elements, sandwich panel filled with a single-layer of APM and thin-wall Al hollow structure filled with free-bonded APM. The compressive testing assessment of hybrid structures based on APM Al foam spheroid elements showed excellent improvements on energy absorption capacity against to Al foam conventional structures. This capacity is led by both the bonding agent and friction effects. The foaming agent applied in this study, white marble, is presented as a functional and low-cost alternative to titanium hydride.

**KEYWORDS:** APMs; Foam; Marble; Porosity; Powder metallurgy; Sandwich Panel

**Citation/Citar como:** Ruiz-Román, J.M.; Sánchez de la Muela, A.; Cambronero, L.E.G.; Ruiz-Bustinza, I. (2020). “Quasi-static and dynamic analysis of single-layer sandwich structures of APM foam spheroid elements in-situ foamed with marble”. *Rev. Metal.* 56(1): e159.https://doi.org/10.3989/revmetalm.159

**RESUMEN:** *Análisis estático y dinámico de estructuras sándwich con núcleo monocapa de esferoides APM espumados in-situ con mármol.* En el presente trabajo se estudia el comportamiento mecánico de las espumas de aluminio mediante la realización de pruebas estáticas y dinámicas de compresión. Una vez que se haya analizado su comportamiento, se debe poder decidir si este material es el adecuado para diferentes tipos de aplicaciones. Se comienza empleando piezas esferoidales de aleación de aluminio AlSi7, espumadas con mármol como agente de soplado, situadas entre dos placas de aluminio fijadas a las bolas con una mezcla formada por resina y un endurecedor. Por otro lado, se preparan otros paneles sándwiches con espumas de aluminio convencionales, adheridos con la misma mezcla a dos placas de aluminio. Estos dos tipos de materiales serán caracterizados mecánicamente.

**PALABRAS CLAVE:** APMs; Espuma; Mármol; Panel Sándwich; Porosidad; Pulvimetalurgia

**ORCID ID:** José M. Ruiz-Román (https://orcid.org/0000-0002-2296-4420); Alejandro Sánchez de la Muela (https://orcid.org/0000-0003-2232-4439); Luis E.G. Cambronero (https://orcid.org/0000-0003-2831-4901); Iñigo Ruiz-Bustinza (https://orcid.org/0000-0002-8571-1105)

## 1. INTRODUCTION

Through millions of years of evolution, nature has optimized while it has expanded the functionality of the synthesized materials. Some natural materials, such as wood, coral and bone matter, have been provided with internal structures based on adjacent hollow cell distributions resulting in lightweight materials with exceptional properties (Woesz *et al.*, 2004). Due to that, scientists has tried to achieve same results designing materials with internal porous structures as an effort to develop of cellular synthetic materials (Sun and Li, 2018).

These kinds of human-made materials are constituted by a network of adjacent polyhedral cells, which respond to a porous configuration, generally, random (Gibson, 2012) and that confers them an improvement of the resistance to compressive loads and a light weight. There two types of materials regarding on their porosity percentage: whether the porosity developed does not exceed 70% this kind of materials is known as porous material and, otherwise, as cellular materials (Sun and Li, 2018). On the one hand depending on the nature of the porous dispersion, two categories of cellular materials are distinguished: firstly, those known as closed-cell porosity, whose cells are similar to polyhedral shapes with solid membranes and are isolated each other. And secondly, whether the solid material of the pore is concentrated in the edges of their cells these structures are known as open-cell porosity (Gibson, 2003) and develop interconnected cells networks. On the other hand, regarding on the geometric space where porosity is contained there are two kind of materials: Two-dimensional (2D) materials, whose porosity is contained in a plane and cells extend orthogonally to this plane, for instance bee-cell cellular and, otherwise, three-dimensional (3D) materials or foams (Sun and Li, 2018). In the literature available, these porous materials are synthesized by ceramic, polymeric or metallic constituents (Woesz *et al*., 2004).

Due to the inherent properties of the internal structure, foams are an attractive alternative for producing rigid and ultralight-weight materials. The applications are limited to impact or crash protection (Radziszewski and Saga, 2017), filtering systems (Hammel *et al.*, 2014), thermal insulation (Liu *et al.*, 2016) and sound damping, energy absorbing packaging (Woesz *et al*., 2004), underwater buoyant structures, aerospace components (Sun and Li, 2018) as in the case of the aircraft flight deck (Elnasri and Zhao, 2016) and in bone implants (prostheses) (Hammel *et al.*, 2014; Sun and Li, 2018).

As was mentioned below, these materials respond to a wide variety of applications. However, the incessant demand for more restrictive needs has motivated the design of new material assemblies capable of responding successfully. An alternative with great potential is the application of foams as a core sandwich panels (Onck, 2003). Sandwich panels consist, mainly, of three layers: a thick core of foam and two solid metal sheets adhered, by their larger surface, to two parallel and centered surfaces of the core (Banhart, 2001; Hohe *et al.*, 2012). Through this structure, the aim is the sheets transmit stress loads along the plane of these and work flexing, while the core acts as a spacer of the sheets according to the desired thickness and absorbs the transverse and shear stresses (Hohe *et al.*, 2012). The adhesion of the solid sheets can be obtained applying an adhesive substance conveniently disposed between foamed core and sheets (Banhart, 2001). Other approach is based on the patent of Baumeister *et al.* (1997), in which metal foam sandwich panels are manufactured by roll bonding technique. When the joint is reached, it is possible to perform deformation tasks in order to configure the final shape desired in the panel. Subsequently, a heat treatment is applied in which the central sheet precursor expands, or foams, while the solid sheets adhered retaining their density. Due to the complexity of the method, it is especially interesting to elaborate an appropriate selection of the metals, in order to avoid the melting of the solid sheets that cover the precursor during the foaming process takes place. As was indicated by Banhart *et al.* (1999), aluminum foam cores can be reinforced with titanium, steel or aluminum solid sheets.

Diverse studies have been developed on the mechanical behavior of metal foam core sandwich panels to both quasi-static and dynamic conditions, while they were exposed to a wide range of temperatures (Hazizan and Cantwell, 2002; Zhu *et al.*, 2018). Hazizan and Cantwell (2002) and Yu *et al.* (2003) studied dynamic response and failure behavior of aluminum foam sandwich structures and reported that the energy absorbed in dynamic tests was lower than that of quasi-static tests. Zhao *et al.* (2007) studied the perforation of a sandwich panel performed through a Hopkinson bar pressure test, and reported the experimental characteristics of the same under impact conditions. Hou *et al.* (2010) also conducted an investigation on the behavior of sandwich panels exposed to ballistic impact conditions, and informed great results in relation to the dynamic energy absorption. Some investigators (Jing *et al.*, 2013) have conducted experimental and numerical studies in accordance with the response of these material assemblies subjected to dynamic test conditions, assessing the response of the panels to energy absorption.

Other studies have reported that the mechanical characteristics of aluminum foams are closely related to the test temperature (Zhu *et al.*, 2018). In the investigations of Aly *et al.* (2007), a ductile behavior could be observed as a result of high temperature exposures. As Xi *et al.* (2015) indicated, both peak load, failure mode and energy absorption are affected by the surrounding temperature. Li *et al.* (2016) agreed that the yield strength value is linearly reduced with the increase in temperature. In subsequent studies (Li *et al.*, 2017), it was found that the energy absorbed, in low-speed and quasi-static tests, met gradual reductions in their value as the temperature increased. These reductions were moderate at temperatures below 200 °C, while they were abrupt for higher temperatures. In successive studies, due to the inherent complexity of high temperature studies, investigations based on numerical models have been implemented (Xi *et al.*, 2017) in order to find a way to predict perforation behaviors under penetration tests. Likewise, there are a diverse studies on the effects of high values of test temperature on foam sandwich panels. These effects have also been investigated in case of reduced values of test temperature (Zhu *et al.*, 2018). In the investigations of Zhu *et al.* (2016), impact tests were performed on an aluminum foam sandwich panel at low temperature (-60 °C, -40 °C and 25 °C). Reporting showed that the panels studied had excellent energy absorption capabilities, compared to sweet steel plates of the same weight even at low temperature. Therefore, aluminum foam sandwich panels could be potential materials for applications such as gearbox protectors, ice hockey helmets, ski protections and boots for high speed sports. Subsequently, Zhu *et al.* (2018) reported a few enhancements as the increase in impact energy absorption and better dynamic responses of Al-foam sandwich panels (AFSP) subjected to low temperature conditions. The deflection obtained at low temperature was lower than that obtained at room temperature due to the yield stress value augment. In addition, results shown the greater number of impacts, the greater effect of low temperature.

Recently, a new type of advanced foams elements known as APMs (Advanced Porous Morphology) have been developed. APMs are defined as hybrid cellular structures developed by the Fraunhofer IFAM center, located in Bremen, Germany (Stöbener *et al.*, 2007). In terms of physical parameters, these new foam elements have near spherical shape and they are constituted by a core of closed-cell porosity surrounded by a thin and solid outer surface. The synthesis process (Fernández *et al.*, 2008; Fernández *et al.*, 2009) is based on the compaction of a mixture of powders, AlSi alloy, and subsequent extrusion of AlSi7 metal alloys with TiH2 as foaming agent. Literature available has proven that other foaming agents such as ZrH2, dolomite and $CaCO_3$ are equally effective (Uzun and Turker, 2014). The foamable precursors are cut in small granules and introduced in a heated oven for foaming (Vesenjak *et al.*, 2013; Ulbin *et al.*, 2014). The density of these foam elements ranges between 500 and 1000 Kg·m-3 depending on the diameter they are found from 5 mm to 15 mm (Stöbener *et al.*, 2007). APM foam elements show exceptional mechanical and thermal properties, highlighting in application such as structural elements for damping energy, as core in diverse assemblies or as a stiffening element (Vesenjak *et al.*, 2013). Their properties depend on the morphology, topology and the base metal they are constituted. Studies on these terms (Ulbin *et al.*, 2014) have reported that the variation of the base Al alloy from AlSi7 to AlSi10 improves both the percentage of spherical-shape porosity content and porosity volume. In other investigations, thermal properties have been explored through predictive numerical models such as the CML (Lattice Monte Carlo) to determine the thermal conductivity (Fiedler *et al.*, 2014) and, by means of thermography of infrared (Krstulović-Opara *et al.*, 2016).

However, one of the greatest advantages of APMs is their application as filler of hollow structures. In general, these structures present two types of porosities: the APM interior voids of (63% -82%) and the interstitial voids between the APM elements (40% -50%) (Vesenjak *et al.*, 2013).

Studies have been carried out to determine the response of these structures exposed to compressive stresses (Hohe *et al.*, 2012; Kovačič and Ren, 2016). Kovačič and Ren (2016), developed a theory to estimate the lower and upper limit values of partial and total porosities in composite materials constituted by APM distributions. This theory includes the error estimation assuming negligible the adhesive phase action in the APM element. Duarte *et al.* (2015), developed compressive tests to metallic tubes filled with APM elements joined by adhesive phases. The results showed a significant influence of the adhesive bond, this effect was a controlled deformation behavior without crack formation and a greater energy absorption capacity. Uzun (2017), conducted experimental studies on the effect of APM elements as filler in hollow tubes subjected to crack mechanisms by compression tests. The quantity of energy absorbed was higher compared to those tubes that did not have APM fillers. Hohe *et al.* (2012), explored the potential application of sandwich panels with a functional gradient core focused on APMs and structures based on hollow sphere assemblies.

From the best of our knowledge, limited studies have been made to investigate the compressive deformation behavior, for single-layer spheroid foam elements as core sandwich panel. In this context, the present investigation is carried out to examine the effect of marble as foaming agent, spheroid foam elements and strain rete on compressive deformation behavior of Al spheroid foam elements as core sandwich panel under different strain rates.

## 2. MATERIALS AND METHODS

### 2.1. Materials

The raw materials should be classified in order to meet a sound understanding of their structural function for hybrid structure assembling.

Base material: The base material used in this study was pre-alloyed commercial pure (99.5%) aluminum powder were supplied by Goodfellow Company. Its chemical composition is presented in Table 1. This Al alloy exhibits excellent stability against atmospheric agents, electrical and high thermal conductivity, as well as excellent deformability.

Foaming Agent: White marble. Marble is a metamorphic rock of great ornamental interest that is formed due to metamorphism of limestones, under conditions of both regional metamorphism and contact, which induce the recrystallization of calcite at high temperature. It is composed mainly of calcite, but may contain other minerals such as mica, dolomite, brucite, vesubianite, wollastonite, diopside, tremoline, graphite or pyrite.

The white marble used in this research work comes from the quarries of Macael (Almería) whose chemical composition is 55.2% CaO, 43.2% $CO_2$, 1.3% MgO, 0.2% $SiO_2$ and 0.1% of others. This rock is supplied in the form of sands with a particle sizes ranging from 0.9 to 1.5 mm. Marble sands were subjected to drying, grinding and sieving processes in order to obtain a powder size of 106–120 microns which conferring an adequate plasticity to the mixture Al-Marble during the extrusion process. Marble replaces conventional foaming agent $TiH_2$ that is nowadays commonly used. This substitute allows avoid using an expensive, reactive and dangerous powder material that release hydrogen ($H_2$) when the foaming process takes place.

Structural Element: The configuration of a hybrid structure made of spheroids foam elements requires structural support elements. In the present study, sandwich panels were manufactured using 1.05 mm thickness commercial pure aluminum face sheets.

The great thermal and mechanical properties of silicon led the selection of the AlSi7 aluminum alloy (Al-7% Si) as the matrix foam. A content of 10% wt of marble powder was carefully mixed with AlSi7, as clustering deteriorates the mechanical properties of the metal foam elements (after the heated extrusion and foaming processes).

### 2.2. Experimental procedures

#### *2.2.1. Preparation of hybrid structures*

The preparation of the hybrid structure was carried out using powder metallurgical method according to the following procedure. Both base material and foaming agent powders were placed and mixed in a crucible for obtaining a homogeneous mixture. This is the most critical preparation stage since it drives the developing desired properties. All aspects of good mixed practices were followed to ensure success. For this step, a V-shape rotating mixer was selected and a nominal speed of 2.1 rad s-1 was used. Mixing of the powder mixture was continued for ensuring the incorporation of marble powders during 30 minutes.

Marble and AlSi7 powders were then cold compacted into a steel cylindrical mold under a continuously pressure of 70 MPa. The as-built green bodies are easily handling and ensures the foaming agent is embedded in the metal matrix without a remarkable open porosity. Absence of open-cell porosity reduces extensively unacceptable oxidation effects during the processing next stage.

Graphite was used as sealant and green compacts are extruded at 520 °C. The temperature applied is close to the AlSi7 aluminum alloy melting point in order to motivate its deformability without applying excessive extruding pressure. The extruded precursor is a cylindrical in shape with 10 mm in diameter and a length between 390 and 500 mm. In the next step the rod is cut in cylindrical pieces of the desired length and heat treated for foaming into an electrical oven at 750 °C. The foaming treatment takes place during a time lapse ranging from 300 to 330 s and below foam elements are air cooled. Depending on the diameter of the extruded precursors, foam elements reach densities of 0.6–0.7 $g \cdot cm^{-3}$.

The manufacturing process last stages consist of assembling 25 individual foam spheroid elements in a 5x5 single layer. The 5x5 layer is the core of the sandwich panel and is adhered to two aluminum parallel sheets (structural sheets). A conventional aluminum foam sandwich panel is configured for comparing results. Sandwich panel foams core, both the foam spheroid elements and conventional

Table 1. Chemical composition of Al-cp alloy (in wt%)

| Aluminum Alloy | | Size | Chemical composition (wt,%) | | | | | | | | |
|---|---|---|---|---|---|---|---|---|---|---|---|
| | | | Si | Fe | Cu | Mn | Mg | Zn | Ti | Other | Al |
| Al99.5 | Tolerences | - | 0.3 | 0.4 | 0.05 | 0.05 | - | 0.1 | 0.03 | 0.03 | Min 99.5 |
| | Goodfellow | 99.5% < 150 μm | 0.04 | 0.1 | - | - | - | - | - | < 0.05 | Rest |

aluminum foams, are adhered to commercially pure aluminum (Al-99.5%) plates by a mixture of resin (EpoFix Resin) and hardener (EpoFix Hardener) with a relation of 25:3. Both of sandwich panel types are shown in Fig. 1 and Fig. 2.

### *2.2.2. Mechanical tests*

Two types of tests were carried out in order to appraise the absorption energy capacity of hybrid structures under compressive conditions. Regarding on the quickness of the energy transmitted there are the following tests: Quasi-static and dynamic compression tests.

- *Quasi-static compression testing*

The quasi-static compression tests were conducted using an INSTRON mechanical test system. Load data were measured through an INSTRON 100 kN load cell with an accuracy of 0.1%, equivalent to 100 N. Displacement data were obtained from the INSTRON measuring actuator system with an accuracy of 0.15 mm and also through a displacement transducer LVDT HBM (range of 40 mm and resolution of 0.04 mm).

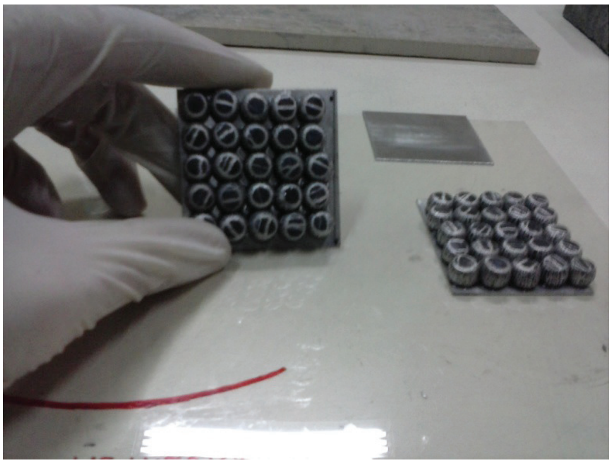

FIGURE 1. Core sandwich panel assembly of 25 spheroidal foam elements bonded to an Al face sheet.

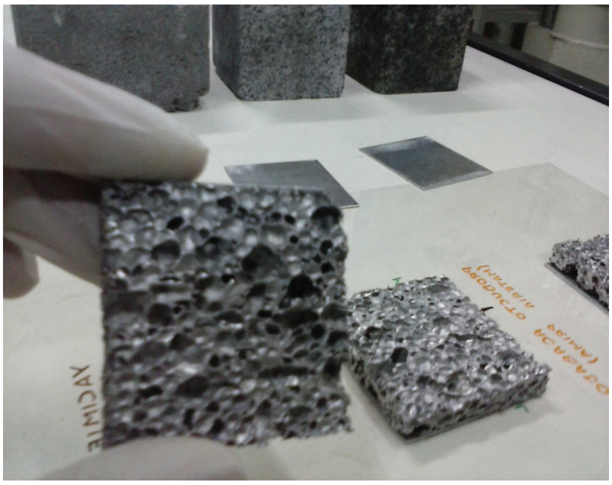

FIGURE 2. Core sandwich panel made of conventional closed-cell Al foam.

- *Dynamic compression testing*

Low-velocity impact tests on single-layer foam sandwich panels were performed by means of a DYNATUP 8500 drop-weight tower. The foam samples were hit orthogonally with a tup piece (striker bar) which is free fall accelerated through a guide. In order to apply a uniform load over entire sample surface it was used a same size penetrator as sample size studied in each case. Two different drop weights were used depending on the type of sample tested, 23.12 kg and 2.2 kg. Another key component of the drop mass configuration is the instrumentation to record the crush event. Loads were measured using a load cell of 50 kN with an accuracy of 0.1% equivalent to 50 N of resolution. Displacements were recorded indirectly through a speed measurement system for obtaining the tup-piece displacement with a resolution of 0.25 mm.

Four mechanical tests were applied to study the both assembly type and shape foam effects on the amount of energy absorption. These tests and their key names are indicated as follows:

- Test 1: Aluminum foam spheroid elements individually tested.
- Test 2: Sandwich panels with a core assembly of 25 aluminum foam spheroids. Each sandwich panel was tested individually.
- Test 3: 25 aluminum foam spheroids confined in a metal mold.
- Test 4: Conventional aluminum foam sandwich panels.

## 3. RESULTS AND DISCUSSION

### 3.1. Quasi-static compression tests

The results of static compression tests for two aluminum foam spheroids tested individually are shown in Fig. 3. The assessments indicate that for a strain rate of 0.8 the spheroids are able to absorb a compressive energy of up to 12 Joules per cubic centimeter. The physical properties of both spheroids are shown in Table 2.

When the APM foam spheroid elements are assembled in an Al sandwich panel, this configuration is able to increase the absorbed energy range from 14 to 16 joules per cubic centimeter (as is shown in Fig. 4). On the one hand, its greater capacity of energy absorption per unit volume is due to the

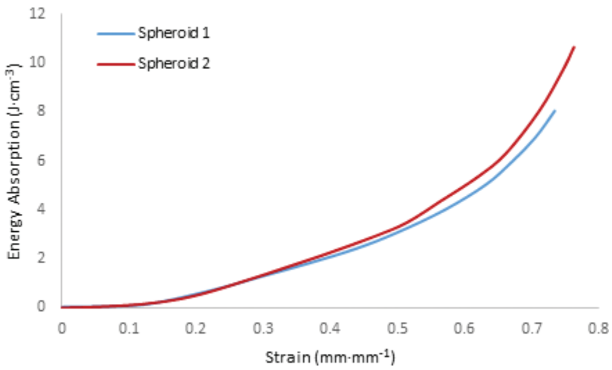


FIGURE 3. Compressive energy absorption-strain curves of spheroid foam elements under quasi-static and high strain rate loading.

TABLE 2. Quasi-static compressive tests. Physical parameters of the spheroids 1 and 2

| Spheroid Id | Height (mm) | Radius (mm) | Weight (g) |
|---|---|---|---|
| Spheroid 1 | 7.01 | 4.14 | 0.248 |
| Spheroid 2 | 7.1 | 4.14 | 0.249 |

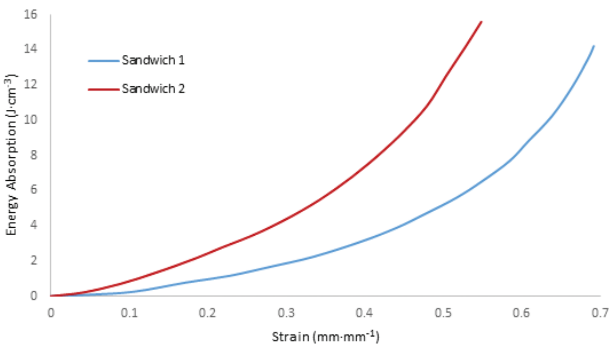


FIGURE 4. Compressive energy absorption-strain curves of sandwich panels under quasi-static and high strain rate loading.

spheroids exert a friction effect when placed next to each other. And on the other hand, the variation of energy absorption is due to the greater quantity of epoxy resin deposited in manufacturing process of the sandwich panel structure 2 (see weight in Table 3). These two parameter caused an increase in the energy absorbed as can be noted. In the Table 3 the physical parameters of the two types of sandwich panel tested are shown.

As a consequence of the resin damping effect observed in Test 2 (shown in Fig. 4) a third test was designed. In this term, the third type of test focused on quantifying how large is the effect of the amount of resin used over the energy absorption capacity. A confined foam spheroids into a metal mold without any type of union between them by means of resin sample a was assembled. In Fig. 5 the result data of

TABLE 3. Quasi-static compressive tests. Physical parameters of the sandwich panels 1 and 2

| Sandwich Panel Id | Surface ($mm^2$) | Height (mm) | Weight (g) |
|---|---|---|---|
| Sandwich 1 | 2500 | 9.26 | 22.499 |
| Sandwich 2 | 2500 | 9.19 | 24.492 |

Test 1, Test 2, Test 3 and Test 4 are shown with the aim of easily comparing its values.

Al foam spheroids individually tested exhibit an energy absorption capacity of up to 12 joules per cubic centimeter. In contrast, spheroid foam elements core sandwich panels present more energy absorption per unit volume thanks to the joint action between the resin and the friction. In these cases, sandwich panel samples reach values ranging from 14 to 16 joules per unit volume.

In Fig. 5 data results of Test 3 (25 confined spheroids into a metal mold) have been analyzed. It can be observed that the energy-strain curves of both Test 2 and Test3 slightly overlap each other ensuring the same behavior in terms of energy and strain achieved. The free-resin configuration of Test 3 samples show the major effect on energy absorption is the friction between spheroid foam elements against each other instead of resin damping effect from Test 2.

The key point that must be highlighted is sandwich panels made of conventional aluminum foam core absorb a much lower amount of energy per unit volume than that absorbed by sandwich panels made of aluminum foam spheroid. So that, it is evidenced that the spheroidal geometry of aluminum foam elements enhance mechanical properties. In addition, this improvement is due to the joint influence of resin and especially of friction in the impact energy damping.

### 3.2. Dynamic compressive tests

Following the same sequence as quasi-static compression tests, the aluminum foam spheroids were tested individually. Their impact behavior results were obtained as are shown in Fig. 6. The energy absorption results of these foam spheroids reach values up to 14 $J \cdot cm^{-3}$ and strains up to 0.6. The data obtained from energy absorption studies are slightly higher than those of the sandwich panels. The rapid deformation level reached, around 0.4, motivate the spheroids were so deformed that the absorption of energy per unit volume grow up dramatically. The physical properties of both foam spheroids are presented in Table 4.

As can be observed in Fig. 7 sandwich panels of 25 aluminum foam spheroids reach values between 7 and 10 $J \cdot cm^{-3}$. Its capacity to absorb energy is due to both the spherical shape of the foam elements and the friction effect of spheroids placed against each

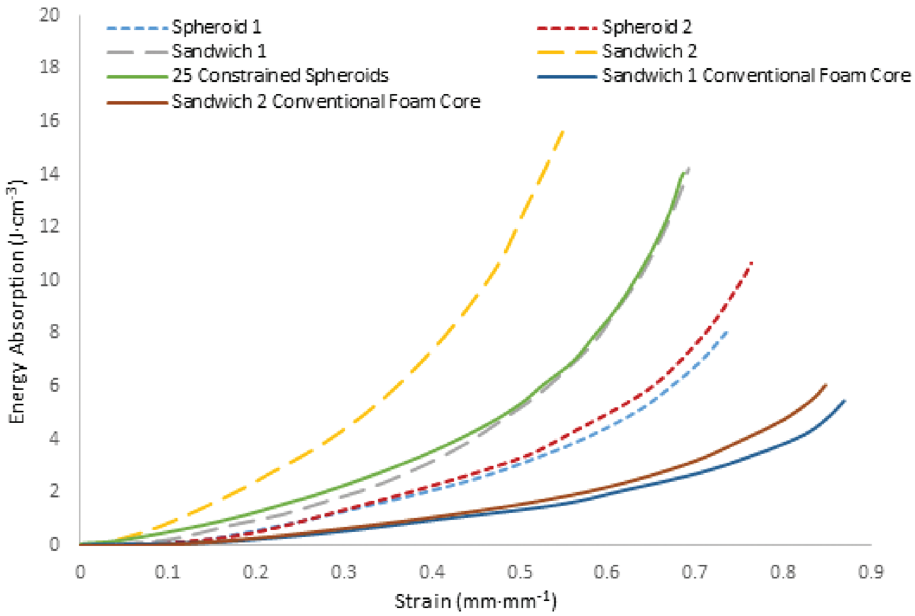


FIGURE 5. Compressive energy absorption-strain curves of foam study samples under quasi-static and high strain rate loading.

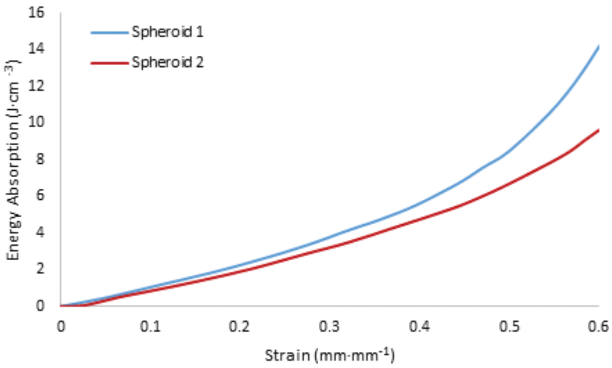


FIGURE 6. Compressive energy absorption-strain curves of spheroid foam elements under dynamic and high strain rate loading.

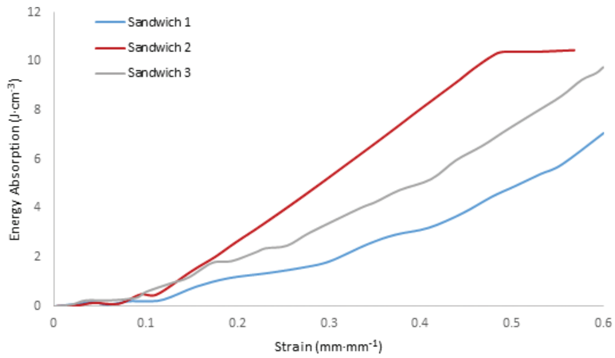


FIGURE 7. Compressive energy absorption-strain curves of sandwich panels under dynamic and high strain rate loading.

TABLE 4. Dynamic compressive tests. Physical parameters of the spheroids 1 and 2

| **Spheroid Id** | **Height (mm)** | **Radius (mm)** | **Weight (g)** | **Velocity ($ms^{-1}$)** |
|---|---|---|---|---|
| Spheroid 1 | 7.66 | 4.14 | 0.249 | 4.02 |
| Spheroid 2 | 7.27 | 4.14 | 0.248 | 4.05 |

TABLE 5. Dynamic compressive tests. Physical parameters of the sandwich panels 1 and 2

| **Sandwich Panel Id** | **Surface ($mm^2$)** | **Height (mm)** | **Weight (g)** | **Velocity ($ms^{-1}$)** |
|---|---|---|---|---|
| Sandwich 1 | 2500 | 9.26 | 22.92 | 3.85 |
| Sandwich 2 | 2500 | 9.19 | 26.252 | 3.80 |
| Sandwich 3 | 2500 | 9.20 | 24.37 | 3.82 |

other as previously mentioned. In case of the sandwich panel 1, the penetrator just hit the center of the panel so that just the centrally located spheroids were testing. For this reason, the values of energy absorption of sandwich panel 1 (7 J·cm$^{-3}$) was lower than in case of sandwich panels 2 and 3. In Table 5, physical parameters of two types of sandwich panel tested are showed.

Similarly, to the quasi-static tests, in Fig. 8 are showed the energy-strain dynamic compression testing curves obtained thus far. This figure allows a smooth comparative of the evolution in absorption energy regarding to different foam structures studied.

The spheroids damp an impact energy of up to 14 J·cm$^{-3}$, this is possible due to the great

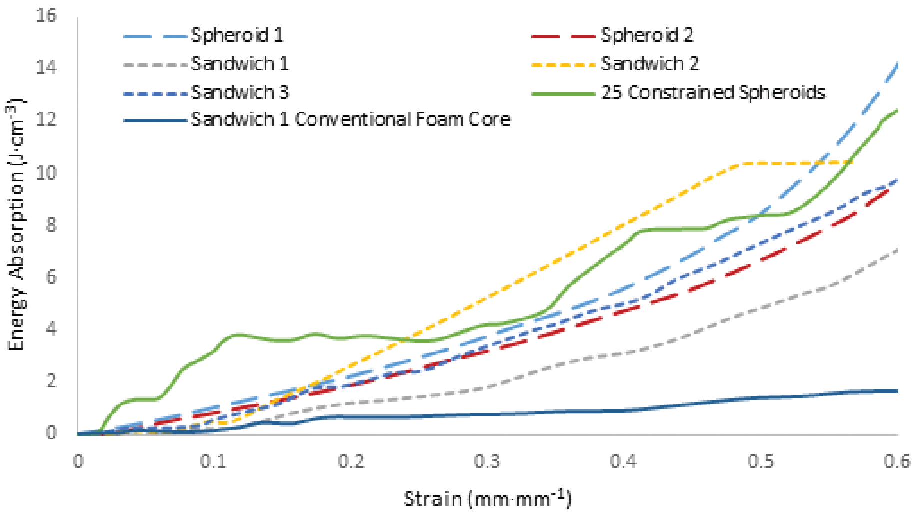


FIGURE 8. Compressive energy absorption-strain curves of foam study samples under dynamic and high strain rate loading.

deformation capacity they undergo as indicated above. Nonetheless, in case of sandwich panels foam spheroids are confined and bonded at top and bottom to structural sheets. During deformation conditions, foam elements undergo friction effects that limit their deformation capacity. This restriction leads reaching maximum values of 10 J·cm$^{-3}$, less energy absorption than un-confined spheroids. However, whether the spheroids are confined without any bonding material between them, the energy absorption achieved values of up to 12 J·cm$^{-3}$. The increase is due to the effect of the rapid deformation suffered by from spheroids under dynamic load conditions.

In any case, this type of hybrid structures based on using Al foam spheroids as sandwich core, allow to reach values of energy absorption against dynamic loads notably higher than those achieved with conventional aluminum foam panels, as is showed in Fig. 8.

## 4. CONCLUSIONS

- The powder metallurgy route for synthesizing aluminum foam spheroids using white marble as a foaming agent, has allowed the obtaining of a competitive product. Therefore at the sight of the results achieved white marble should be considered as a reasonable alternative to titanium hydride.
- The hybrid structures of sandwich panels based on Al foam spheroids exhibit a great energy absorption capacity. That capacity is remarkably superior comparing with conventional Al foam core sandwich structures, subjected to same quasi-static or low-dynamic compressive conditions.
- The deformation processes of the hybrid structures, in terms of energy-strain, is motivated by two parameters: friction and bonding agent. The foam spheroids elements friction effect increases the impact energy absorption and this capacity is complemented by the bonding agent effect.

As future lines of research:

- Different kinds of manufacturing configurations of hybrid sandwich structures should be addressed.
- The studies should focus on the mechanical compression behavior of sandwich panel stacks with several layers of these aluminum foam spheroid. Probably seeing for the possible improvement of designing cumulative panels.
- The exploration of the different types of binders on bonding of alternate layers of Al conventional foam core sandwich panels combined with layers of sandwich panels based on Al foam spheroids cores.

## REFERENCES


Aly, M.S. (2007). Behavior of closed cell aluminium foams upon compressive testing at elevated temperatures: Experimental results. *Mater. Lett.* 61 (14–15), 3138–3141. https://doi.org/10.1016/j.matlet.2006.11.046.

Baumeister J., Banhart, J., Weber, M. (1997). Metallischer Verbundwerkstoff und Verfahren zu seiner Herstellung, Patente Alemana DE 4426627.

Banhart, J., Ashby, M., Fleck, N. (1999). *Metal foams and porous metal structures*. Conference on Metal Foams and Porous Metal Structures, 14th - 16th, Verlag MIT Publishing, Bremen.

Banhart, J. (2001). Manufacture, characterisation and application of cellular metals and metal foams. *Prog. Mater. Sci.* 46 (6), 559–632. https://doi.org/10.1016/S0079-6425(00)00002-5.

Duarte, I., Vesenjak, M., Krstulović-Opara, L., Ren, Z. (2015). Compressive performance evaluation of APM

(Advanced Pore Morphology) foam filled tubes. *Compos. Struct.* 134, 409–420. https://doi.org/10.1016/j.compstruct.2015.08.097.
Elnasri, I., Zhao, H. (2016). Impact perforation of sandwich panels with aluminum foam core: a numerical and analytical study. *Int. J. Impact Eng.* 96, 50–60. https://doi.org/10.1016/j.ijimpeng.2016.05.013.
Fernández, P., Cruz, L.J., Coleto, J. (2008). Procesos de fabricación de metales celulares. Parte I: Procesos por vía líquida. *Rev. Metal.* 44 (6), 540–555. https://doi.org/10.3989/revmetalm.0767.
Fernández, P., Cruz, L.J., Coleto, J. (2009). Procesos de fabricación de metales celulares. Parte II: Vía sólida, deposición de metales, otros procesos. *Rev. Metal.* 45 (2), 124–142. https://doi.org/10.3989/revmetalm.0806.
Fiedler, T., Sulong, M.A., Vesenjak, M., Higa, Y., Belova, I.V., Öchsner, A., Murch, G.E. (2014). Determination of the thermal conductivity of periodic APM foam models. *Int. J. Heat Mass Tran.* 73, 826–833. https://doi.org/10.1016/j.ijheatmasstransfer.2014.02.056.
Gibson, L.J. (2003). Cellular solids. *MRS Bull.* 28 (4), 270–274. https://doi.org/10.1557/mrs2003.79.
Gibson, L.J. (2012). The hierarchical structure and mechanics of plant materials. *J. Roy. Soc. Interface* 9 (76), 2749–2766. https://doi.org/10.1098/rsif.2012.0341.
Hammel, E.C., Ighodaro, O.R., Okoli, O.I. (2014). Processing and properties of advanced porous ceramics: An application-based review. *Ceram. Int.* 40 (10), 15351–15370.
Hazizan, M.A., Cantwell, W.J. (2002). The low velocity impact response of foam-based sandwich structures. *Compos. Part B-Eng.* 33 (3), 193–204. https://doi.org/10.1016/S1359-8368(02)00009-4.
Hohe, J., Hardenacke, V., Fascio, V., Girard, Y., Baumeister, J., Stöbener, K., Weise, J., Lehmhus, D., Pattofatto, S., Zeng, H., Zhao, H., Calbucci, V., Rustichelli, F., Fiori, F. (2012). Numerical and experimental design of graded cellular sandwich cores for multi-functional aerospace applications. *Mater. Design* 39, 20–32. https://doi.org/10.1016/j.matdes.2012.01.043.
Hou, W., Zhu, F., Lu, G., Fang, D.N. (2010). Ballistic impact experiments of metallic sandwich panels with aluminium foam core. *Int. J. Impact Eng.* 37 (10), 1045–1055. https://doi.org/10.1016/j.ijimpeng.2010.03.006.
Jing, L., Xi, C., Wang, Z., Zhao, L. (2013). Energy absorption and failure mechanism of metallic cylindrical sandwich shells under impact loading. *Mater. Design* 52, 470–480. https://doi.org/10.1016/j.matdes.2013.05.090.
Kovačič, A., Ren, Z. (2016). On the porosity of advanced pore morphology structures. *Compos. Struct.* 158, 235–244. https://doi.org/10.1016/j.compstruct.2016.09.046.
Krstulović-Opara, L., Vesenjak, M., Duarte, I., Ren, Z., Domazet, Ž. (2016). Infrared thermography as a method for energy absorption evaluation of metal foams. *Mater. Today-Proc.* 3 (4), 1025–1030. https://doi.org/10.1016/j.matpr.2016.03.041.
Li, Z., Chen, X., Jiang, B., Lu, F. (2016). Local indentation of aluminum foam core sandwich beams at elevated temperatures. *Compos. Struct.* 145, 142–148. https://doi.org/10.1016/j.compstruct.2016.02.083.
Li, Z., Zheng, Z., Yu, J., Lu, F. (2017). Deformation and perforation of sandwich panels with aluminum-foam core at elevated temperatures. *Int. J. Impact Eng.* 109, 366–377. https://doi.org/10.1016/j.ijimpeng.2017.07.001.
Liu, R., Xu, T., Wang, C.A. (2016). A review of fabrication strategies and applications of porous ceramics prepared by freeze-casting method. *Ceram. Int.* 42 (2), 2907–2925. https://doi.org/10.1016/j.ceramint.2015.10.148.
Onck, P.R. (2003). Scale effects in cellular metals. *MRS bull.* 28 (4), 279–283. https://doi.org/10.1557/mrs2003.81.
Radziszewski, L., Saga, M. (2017). Modeling of non-elastic properties of polymeric foams used in sports helmets. *Procedia Engineer.* 177, 314–317. https://doi.org/10.1016/j.proeng.2017.02.231.
Stöbener, K., Baumeister, J., Rausch, G., Busse, M. (2007). Metal foams with advanced pore morphology (APM). *High Temp. Mat. Pr-ISR* 26 (4), 231–238. https://doi.org/10.1515/HTMP.2007.26.4.231.
Sun, Y., Li, Q.M. (2018). Dynamic compressive behaviour of cellular materials: A review of phenomenon, mechanism and modelling. *Int. J. Impact Eng.* 112, 74–115. https://doi.org/10.1016/j.ijimpeng.2017.10.006.
Ulbin, M., Borovinšek, M., Higa, Y., Shimojima, K., Vesenjak, M., Ren, Z. (2014). Internal structure characterization of AlSi7 and AlSi10 advanced pore morphology (APM) foam elements. *Mater. Lett.* 136, 416–419. https://doi.org/10.1016/j.matlet.2014.08.056.
Uzun, A., Turker, M. (2014). The effect of production parameters on the foaming behavior of spherical-shaped aluminum foam. *Mater. Res.* 17 (2), 311–315. https://doi.org/10.1590/S1516-14392014005000006.
Uzun, A. (2017). Compressive Crush Performance of Square Tubes Filled with Spheres of Closed-Cell Aluminum Foams. *Arch. Metall. Mater.* 62 (3), 1755–1760. https://doi.org/10.1515/amm-2017-0267.
Vesenjak, M., Borovinšek, M., Fiedler, T., Higa, Y., Ren, Z. (2013). Structural characterisation of advanced pore morphology (APM) foam elements. *Mater. Lett.* 110, 201–203. https://doi.org/10.1016/j.matlet.2013.08.026.
Woesz, A., Stampfl, J., Fratzl, P. (2004). Cellular solids beyond the apparent density–an experimental assessment of mechanical properties. *Adv. Eng. Mater.* 6 (3), 134–138. https://doi.org/10.1002/adem.200300529.
Xi, H., Tang, L., Yu, J., Zhang, X., Xie, B., Liu, Y., Jiang, Z., Liu, Z. (2015). Low velocity penetration mechanical behaviors of aluminum foam sandwich plates at elevated temperature. *Int. J. Struct. Stab. Dy.* 15 (4), 1450063. https://doi.org/10.1142/S0219455414500631.
Xi, H., Tang, L., Luo, S., Liu, Y., Jiang, Z., Liu, Z. (2017). A numerical study of temperature effect on the penetration of aluminum foam sandwich panels under impact. *Compos. Part B-Eng.* 130, 217–229. https://doi.org/10.1016/j.compositesb.2017.07.044.
Yu, J.L., Wang, X., Wei, Z.G., Wang, E.H. (2003). Deformation and failure mechanism of dynamically loaded sandwich beams with aluminum-foam core. *Int. J. Impact Eng.* 28 (3), 331–347. https://doi.org/10.1016/S0734-743X(02)00053-2.
Zhao, H., Elnasri, I., Girard, Y. (2007). Perforation of aluminium foam core sandwich panels under impact loading - An experimental study. *Int. J. Impact Eng.* 34 (7), 1246–1257. https://doi.org/10.1016/j.ijimpeng.2006.06.011.
Zhu, L., Guo, K., Li, Y., Yu, T.X., Zhou, Q. (2016). Impact Resistance of Aluminium Foam Sandwich Plate under Low Temperatures. The 2nd International Conference in Sports Science & Technology, Singapore.
Zhu, L., Guo, K., Li, Y., Yu, T.X., Zhou, Q. (2018). Experimental study on the dynamic behaviour of aluminium foam sandwich plates under single and repeated impacts at low temperature. *Int. J. Impact Eng.* 114, 123–132. https://doi.org/10.1016/j.ijimpeng.2017.12.001.